NASA Contractor Report 181908

THREE COMPONENT LASER DOPPLER MEASUREMENTS IN AN AXISYMMETRIC JET

John M. Kuhlman and Robert W. Gross
West Virginia University
Mechanical and Aerospace Engineering Department
Morgantown, West Virginia

October 1989

Prepared for
NASA Langley Research Center
under NAG1-748

National Aeronautics and
Space Administration

Langley Research Center
Hampton, Virginia 23665-5225

THREE COMPONENT LASER DOPPLER MEASUREMENTS IN AN AXISYMMETRIC JET

by

John M. Kuhlman and Robert W. Gross
West Virginia University
Mechanical and Aerospace Engineering Department
Morgantown, WV
26506

ABSTRACT

A three-component laser doppler anemometer (LDA) has been used to acquire a detailed set of three-dimensional mean and fluctuating velocity measurements in a low-speed air jet entering a stagnant ambient, over the first 20 jet exit diameters along the jet trajectory. These data are physically consistent with previous measurements in axisymmetric jets. The relative difficulty of obtaining three-dimensional and two-dimensional LDA data is briefly discussed.

DESCRIPTION OF EXPERIMENTAL FACILITY AND PROCEDURE

The LDA system used is a commerical five beam DANTEC system with the general layout described by Buchave (ref. 1). Standard DANTEC 55X modular optics and a series 2000 5W Spectra Physics argon ion laser are mounted to a 3-D, computer-controlled traversing system, as is indicated schematically in Figure 1. This traverse uses a pair of 45 degree mirror cubes for each optical train so that only the front lenses are traversed vertically. This leads to a lighter, less expensive traverse, but adds to the difficulty of maintaining optical alignment and coincidence of the probe volumes, from the independent one-channel and two-channel anemometers which form the 3-D system. For the present work front lenses with a focal length of 0.6 m are used, so the angle

between the two separate optical trains is equal to 60°. This large angle helps greatly to improve accuracy of the 3-D velocity measurements, as discussed by Meyers (ref. 2).

Three separate LDA channels are formed (by use of color separation) into 488 nm and 514.5 nm wavelength beams, which form orthogonal fringes by means of a standard DANTEC two-channel optical train, shown on the right-hand side of Figure 1. The vertical (Z) velocity component is measured using the 488 nm beam, while the 514.5 nm beam mesures a velocity component at right angle to the optical axis, in a horizontal plane (i.e., inclined 30° above the Y axis defined in Figure 1). The third LDA channel uses the 476 nm wavelength beam from the Argon ion Laser, which is sent to the DANTEC single-channel optical train which is indicated on the left-hand side of Figure 1. This LDA channel measures a velocity component in a horizontal plane at an angle 30° below the Y axis in Figure 1. This 476 nm beam generally yields the weakest of the three signals. Orthogonal horizontal (X-Y) velocity components are computed by a vector transformation from the non-orthogonal to the orthogonal coordinate system.

The two-channel and one-channel LDA systems both use standard DANTEC 55x modular LDA optics, which includes a beam splitter, a 55N10 Bragg cell frequency shifter, a beam displacer, a backscatter section, photomultiplier optics and photomultiplier tube(s), a pinhole section, beam translator, and beam expander. Frequency shifting allows measurements in reversing flows, while the beam expanders increase signal-to-noise ratio.

The beams exiting each of the separate LDA systems are focused to a single point, as indicated in Figure 1, using two pairs of front surfaced mirrors mounted at 45° angles. The bottom, stationary mirror cubes deflect the horizontal, parallel beams exiting the beam expander sections vertically

onto the second pair of 45° mirror cubes. These mirrors are mounted at ±30° angles from the X axis, and have the 600 mm focal length front lenses mounted so as to focus all beams down to the same probe volume, as indicated in Figure 1. These top mirrors must be adjusted manually (pan and tilt) to obtain coincidence of the probe volumes of the two channel LDA (right side of system) and the single channel LDA (left side). This adjustment is difficult, but is necessary to ensure that LDA signals on all three channels are due to the same seed particle. Also, these top mirrors are traversed vertically with respect to the rest of the 3-D LDA system to traverse the probe volumes in the Z direction. The entire 3-D LDA system is traversed in the X and Y directions.

Output of the photomultiplier tubes from the three separate LDA channels are sent to three DANTEC 55L90A counter processors, operated in the combined mode. Output from the three counter processors goes to a DANTEC 57G20 buffer interface and 57G149 coincidence filter, which accept validated data from each channel, check that the three separate velocity measurements from each channel all were measured within a user-selectable time window which defines coincidence of the data, and measure the time between each set of measurements of the three velocity components. Validated, coincident data and the measured sample interval time are sent to a PDP 11/23 microcomputer for storage. The maximum total data throughput is nominally 6 to 10 kHZ. The entire system (data acquisition and traversing) is controlled by the DANTEC LDAMAP menu-driven interactive software.

The jet facility consists of an air compressor which supplies air through a pressure regulator, oil separator, filters, control valve, and rotameter to a 120:1 area ratio contraction which exits to a 0.415 inch diameter jet exit pipe which is nominally 45 jet diameters in length. A schematic of the jet facility

is shown in Figure 1. For the present nominal exit Reynolds number of 23,000 based on jet exit diameter, it is expected that exit velocity profiles should correspond to fully developed turbulent pipe flow. The jet enters near the centerline of a 18" x 20" cross section low speed wind tunnel. The jet enters the tunnel test section transverse to the tunnel axis. For the present study, no crossflow has been used; the tunnel has been used simply to contain the jet flow seed particles. The tunnel is fitted with a vertical glass side, to allow optical access for the LDA system.

The jet flow has been seeded with 0.5-4 μm diameter glass microbeads from a cylindrical fluidized bed feeder which is fitted with an electric shaker, to ensure a uniform seed rate. The maximum particle diameter of 4 μm is estimated to be capable of following the flow up to frequencies of 2-3 kHz, based upon the work of Hjelmfelt and Mockros (ref. 3). Since the total data transfer rate to the microcomputer is limited to a maximum of no more than 10 kHz, this frequency response for one channel is judged to be adequate for the present system. Seed rate is adjusted to achieve as high a validated data rate as possible, up to about 1 kHz on each channel, in an effort to minimize any interface buffer memory overflows. Minimum data rates, near the jet edges for lateral traverses, are about 300 Hz on each channel. Data validation rates vary from about 60% to about 10%, depending on location and velocity channel. These overall validated data rates yield calculated data densities on the order of 0.3-1, based on the computed Taylor micro time scale (ref. 4). Data files obtained in the current study at each location consist of 2816 measurements of each of the three velocity components, plus the sample interval time since the last validated coincident set of three velocity component measurements. For this study, coincidence between measured velocity components has been defined to occur when all three laser velocimeter

channels send a validated velocity measurement to the buffer within 30μs of one another. This is approximately twice the length of a typical burst on any of the three channels.

Data is reduced using techniques discussed by Edwards (ref. 4) and Meyers (ref. 5). The "tails" of frequency histograms are deleted for each channel, to eliminate spurious data. Approximately one percent of data for each channel is eliminated this way. Also, sample interval time weighting is used to calculate average velocities, RMS values, and velocity cross-correlation distributions. Data reduction is accomplished by uploading data files from the PDP-11/23 to the College of Engineering VAX 11-785 computer.

Results have been obtained for X/D $\leq$20 at a nominal jet Reynolds number of 23,000 based upon jet exit diameter. Three-dimensional mean velocity distributions will be presented, as well as 3-D RMS fluctuation and velocity cross-correlation distributions. Measured results generally compare favorably with typical previous measurements in axisymmetric jets (e.g. refs. 6,7).

RESULTS

Data to be presented consist of a series of seven lateral traverses across the jet axis in the horizontal or vertical directions, at various axial locations, and three traverses in the direction of the jet centerline. At each point the reduced data consist of the calculated mean and RMS velocity components, and the calculated velocity cross-correlations. Results for the lateral surveys across the jet are presented in Figs. 2-10, while the jet centerline traverses are presented in Figs. 11-19. Note that all of these results are essentially three-dimensional measurements in what is basically a two-dimensional (X,R) mean flow field. Mean and RMS velocities are in units of m/s, while cross-correlation results are in units of $(m/s)^2$.

Mean axial velocity profiles versus Y or Z (Fig. 2) clearly indicate the

widening of the jet as X increases, as well as the decay of centerline mean axial velocity. (The coordinate system used in the present study is defined in Fig. 1.) Vertical and lateral profiles of mean axial velocity are essentially identical at the same axial locations, indicating the axisymmetry of the flow. Symmetry of each individual profile in Fig. 2 also is indicative of axisymmetry of the flow.

Lateral profiles of mean radial velocity (Fig. 3) are all essentially antisymmetric. Peak radial velocities are on the order of 1-2 m/s or only about 5-8 percent of the mean axial velocities shown in Fig. 2.

Note that separate traverses were made to measure axial velocity (Figure 2) and radial velocity (Figure 3) at the same X location, but traversing through the jet centerline horizontally (versus Y) and vertically (versus Z). The fact that these measurements agree not only indicates the axisymmetry of the flow, but also confirms the accuracy of the calculated horizontal X and Y velocities, which have been found through vector addition of the X and Y velocity components from the two measured non-orthogonal, horizontal velocity components.

The third mean velocity component (Fig. 4) should be zero in this axisymmetric jet flow, since it is the swirl (circumferential) velocity. Generally, measured mean circumferential velocities are no larger than ±0.5 m/s. Magnitudes decrease as X increases, perhaps partly due to the traverses nearer to the jet exit not having been exactly through the jet midplane.

Lateral profiles of measured RMS axial, radial, and circumferential turbulent velocities are presented in Figs. 5-7, respectively. The axial RMS velocity is consistently about 30% larger than the other two components, which tend to be of about the same magnitude. This behavior is expected on physical grounds (ref. 8). All three fluctuating velocity components display a

double-peaked behavior nearer to the jet exit, which tends to smooth out and disappear for larger X values.

Lateral profiles of fluctuating velocity cross-correlations (Figs. 8-10) indicate the expected good correlation between axial (u') and radial (v') fluctuations (Fig. 8), with little or no correlation between the circumferential velocity fluctuation and either axial or radial fluctuations. Axial-radial correlation profiles are antisymmetric, as expected. Magnitudes of these turbulent fluctuation magnitudes (Figs. 5-10) are consistent with other earlier measurements in axisymmetric jets (refs. 6,7).

Results for traverses along the jet axis (Figs. 11-19) clearly indicate the centerline mean velocity decay (Fig. 11), while the two remaining mean velocities (Figs. 12, 13) are essentially zero. Turbulent RMS velocity fluctuations in the axial, lateral, and vertical directions (Figs. 14-16) all initially increase near the jet exit and then begin to decay. As expected, the fluctuating velocity cross-correlations are not significant along the jet centerline (Figs. 17-19). Negative values of $\overline{u'v'}$ (Fig. 17) for the centerline travese taken at Y/D = 0 for X/D $\leq$ 7, and positive $\overline{u'v'}$ values for the traverse taken at Y/D = 0.38 for X/D $\leq$ 5, are explained by a slight bending of the jet axis away from the X-direction towards the positive Y-direction, so that the jet flow may exit from the tunnel.

Finally, it should be remarked that the scatter in measured circumferential velocity of approximately $\pm$0.5 m/s (Fig. 4) is believed to be representative of the typical measurement uncertainty for mean velocity in the present study. This corresponds to errors of between 1.5 and 3% in the mean axial velocity. However, percent uncertainty is considerably larger for mean radial velocity, since it is smaller in magnitude.

TWO-DIMENSIONAL VERSUS THREE-DIMENSIONAL MEASUREMENTS

One of the goals of the present work was to successfully obtain three-dimensional velocity data in a low-speed, axisymmetric air jet. A second goal was to assess the relative difficulty of obtaining three-dimensional data, as compared to making simultaneous measurements of two velocity components. Even with the commercially available 3-D system used in the present work, it has been found that the measurement of a third velocity component causes a significant increase in difficulty. This is essentially due to the difficulty in obtaining and maintaining coincidence fo the probe volumes of all three LDA channels.

As explained by Meyers (ref. 2), this is partly due to the need for a large angle between the two separate LDA systems to accurately resolve the two orthogonal horizontal velocity components, which leads to a relatively large traversing system and two separate sets of lenses. As a result there is significant difficulty in achieving and maintaining adequate system alignment to match the three probe volume locations to ensure coincident measurements of all three velocity components. With the present 3-D system, this is a time consuming, nearly "hit-or-miss" process of optimizing the fringe intensities and shapes of the five laser beams (3 beams for the 2-D LDA, and 2 additional beams for the 1-D LDA), when passed through a pinhole placed in the region where flow measurements are desired. This iterative process of obtaining coincident probe volumes is made somewhat easier by mounting the pinhole to a manual X-Y-Z traverse, but still often takes about as long as the actual data acquisition process itself. Also, temperature changes in the lab often will destroy this system alignment from day to day, due to the thermal expansion of the traverse and top mirror cubes. It is felt that a lack of adequate coincidence of the probe volumes for the two separate LDA systems is one of

the key limitations to data obtained using the present system. Possibly, the development of an automated traverse for the pinhole and automated drives for the adjustable mirror cubes would help to shorten the time required to obtain coincident three channel data. Also, a combination of a conventional 2-D fringe type LDA system, and Fabry-Perot interferometry to measure the "spanwise" or on-axis velocity component, as described in ref. 9, shows promise for overcoming these limitations since all three channels are focused on the probe volume by the same lens. However, this 3-D anemometer system is at present limited to mean flow measurements, at least for the on-axis velocity component. Finally, in applications where only values of the three mean velocity components are of interest, it is possible that it may be easier to obtain adequate 3-D mean flow data, by relaxing somewhat the requirement for coincidence of the probe volumes for 3-D LDA configurations similar to the present system.

CONCLUSION

A set of three-component LDA data has been obtained in a low speed, axisymmetric air jet entering a stagnant ambient. Mean and turbulent velocity results are consistent with other published results for turbulent, circular jets. For the present three-component LDA system, it is considerably more difficult to obtain physically meaningful three-component data than two-component data. This is largely due to difficulty in achieving and maintaining coincidence of the three separate probe volumes.

REFERENCES

1. Buchave, P., "Three-component LDA Measurements," DISA Information No. 29, Jan. 1984, pp. 3-9.

2. Meyers, J.F., "The Elusive Third Component," Proceedings of Int'l. Symposium on Laser Anemometry, ASME FED-Vol. 33, A. Dybbs & P.A.Pfund, editors, 1985, pp. 247-254.

3. Hjelmfelt, A.T., Jr. and Mockros, L.F., "Motion of Discrete Particles in a Turbulent Fluid," Applied Science Research, Vol. 16, 1966, pp. 149-161.

4. Edwards, R.V., editor, "Report of the Special Panel on Statistical Particle Bias Problems in Laser Anemometry," ASME J. Fluids Engineering, Vol. 109, June 1987, pp. 89-93.

5. Meyers, J.F., "Laser Velocimeter Data Acquisition and Real Time Processing Using a Microcomputer," presented at 4th Int'l. Symposium on Applications of Laser Anemometry to Fluid Mechanics, Lisbon, Portugal, July 11-14, 1988.

6. Hussein, H.J., George, W.K., and Capp, S.P., "Comparison Between Hot-Wire and Burst-Mode LDA Velocity Measurements in a Fully-Developed Turbulent Jet," Paper AIAA-88-0424, presented at AIAA 26th Aerospace Sciences Meeting, Reno, NV, Jan. 11-14, 1988.

7. Rajaratham, N., Turbulent Jets, Vol. 5, Developments in Water Science, Elsevier Publishing Co., NY, 1976, pp. 27-49.

8. Tennekes, H. and Lumley, J. L., A First Course in Turbulence, MIT Press, Cambridge, MA, 1972, pp. 74-75.

9. Seasholtz, R. G. and Goldman, L. J., "Combined Fringe and Fabry-Perot Anemometer for Three Component Velocity Measurements in Turbine Stator Cascade Facility," Paper 13, AGARD-CP-399, Advanced Instrumentation for Aero Engine Components, 1986.

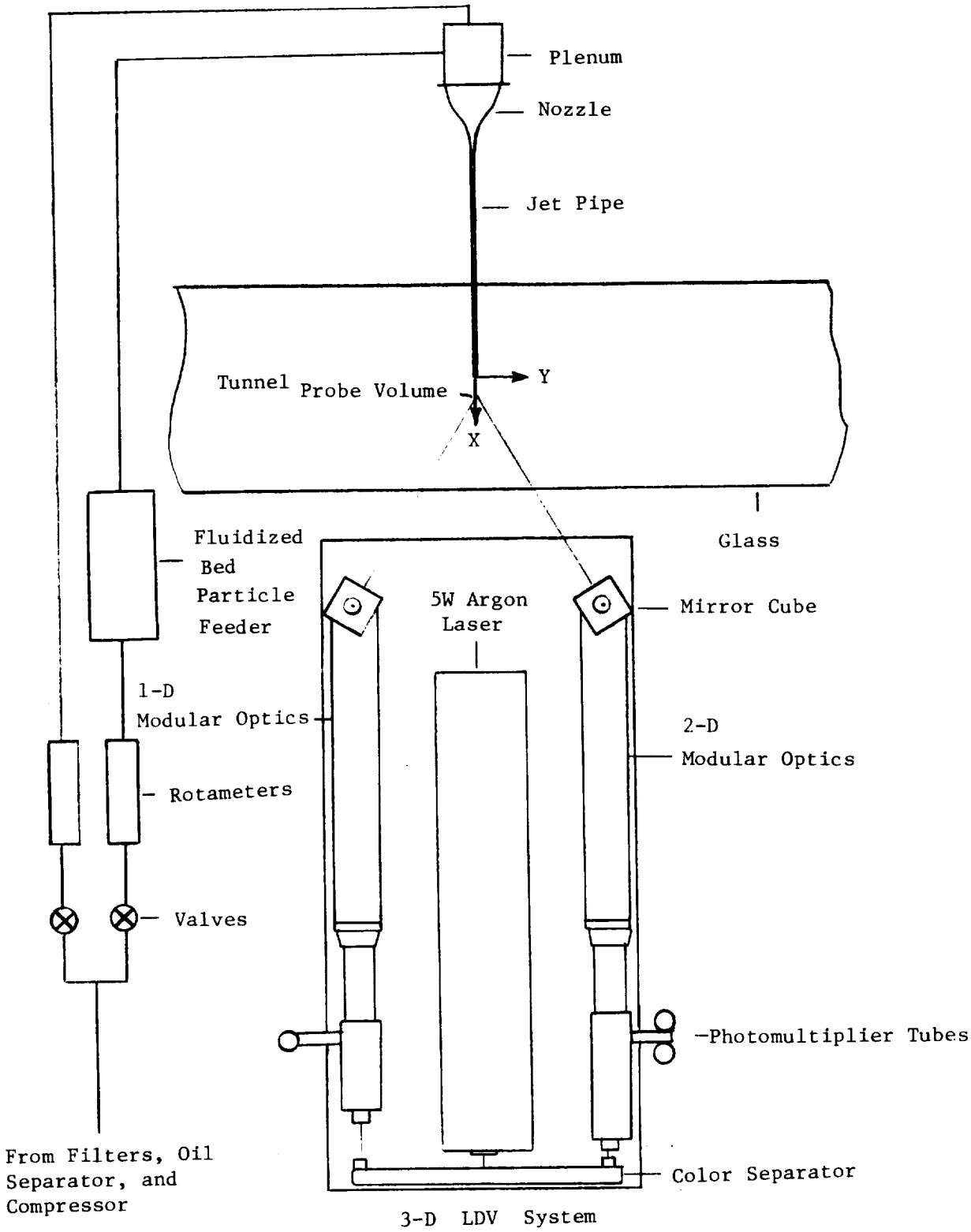

Fig. 1 Schematic of jet flow facility

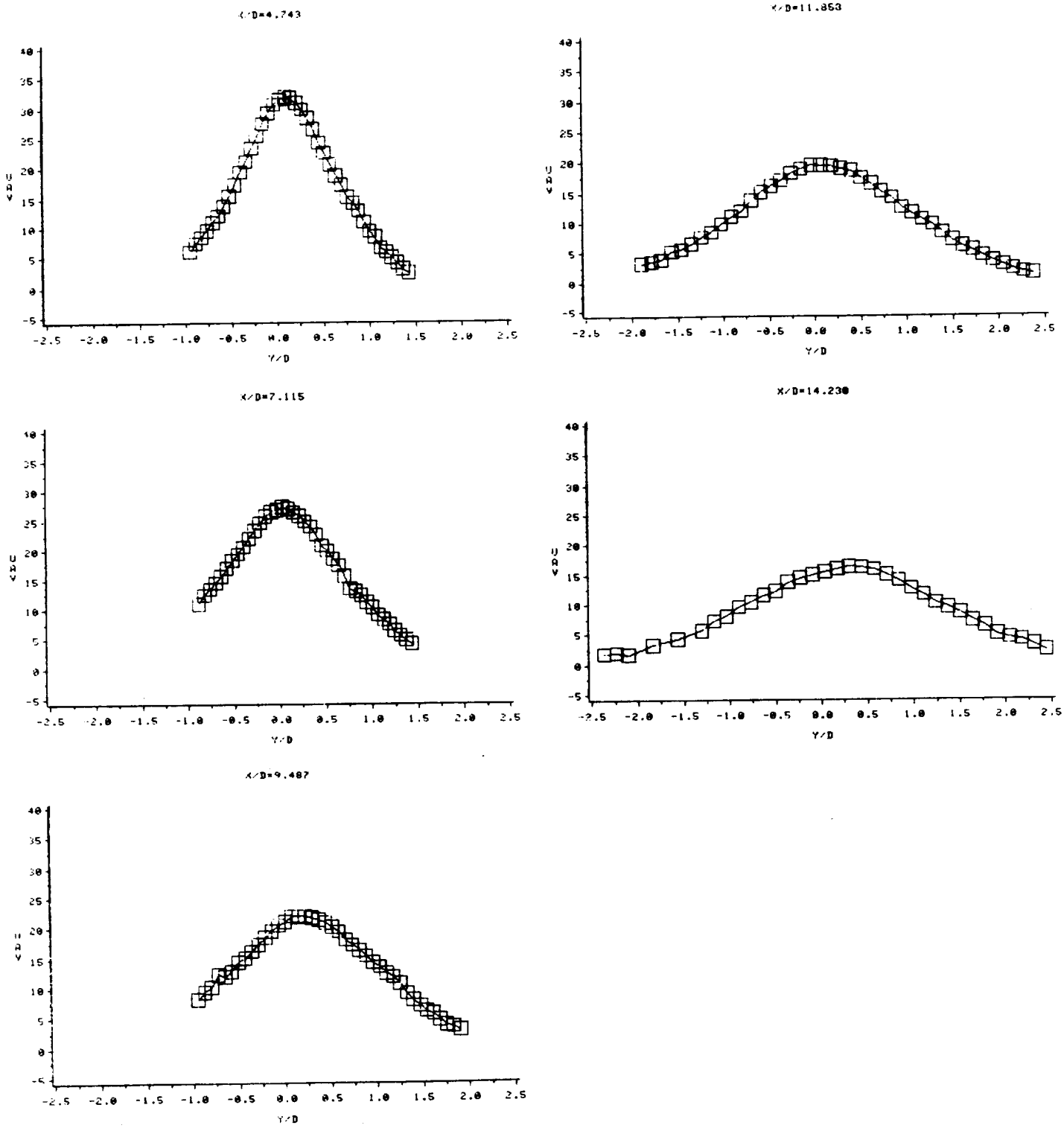

Fig. 2 Lateral profiles of mean axial velocity, U

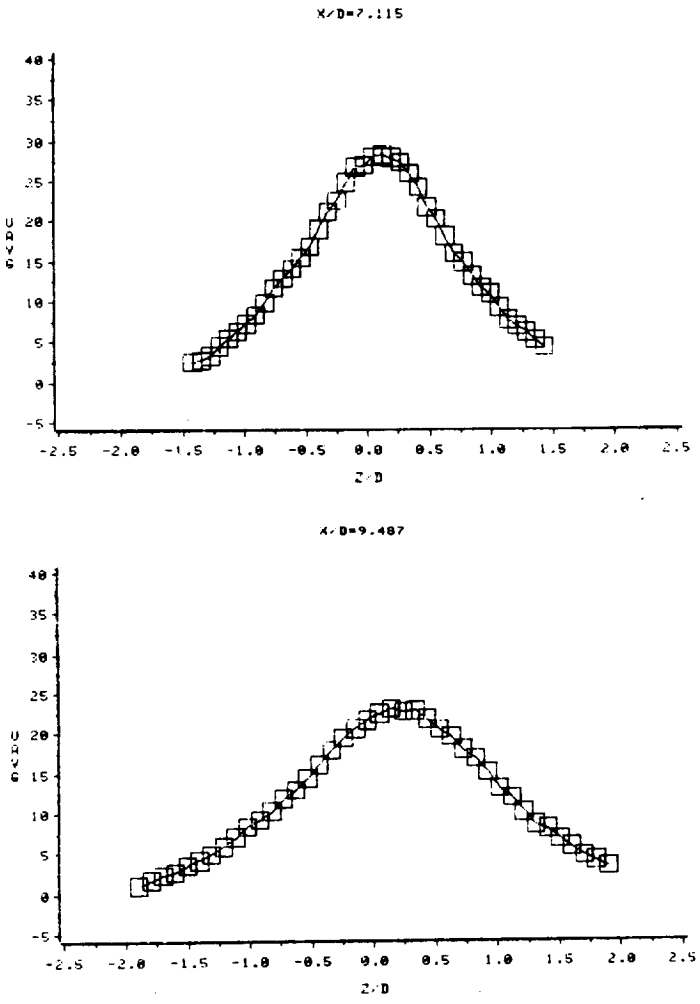

Fig. 2 Lateral profiles of mean axial velocity, U

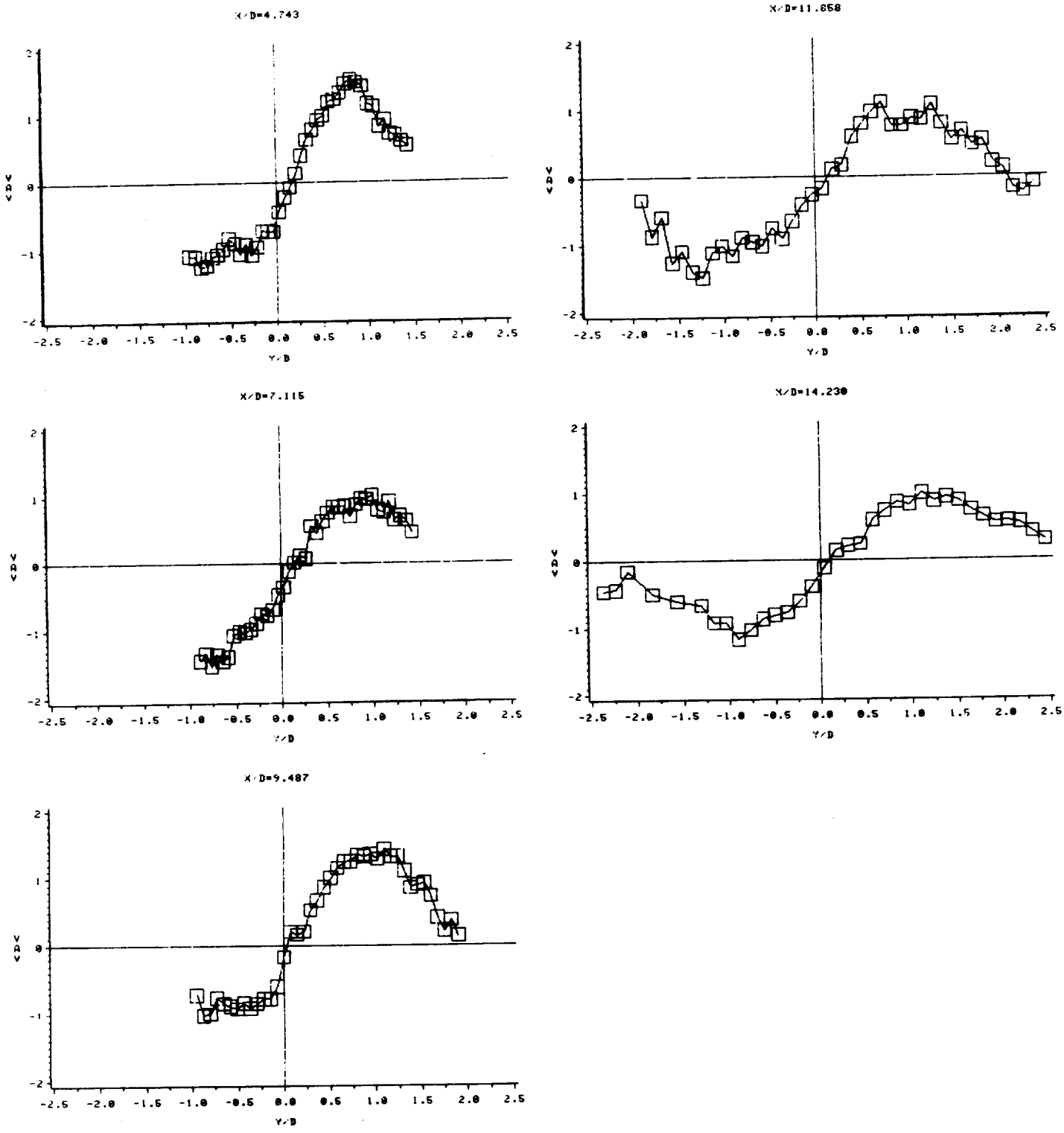

Fig. 3 Lateral profiles of mean radial velocity, V

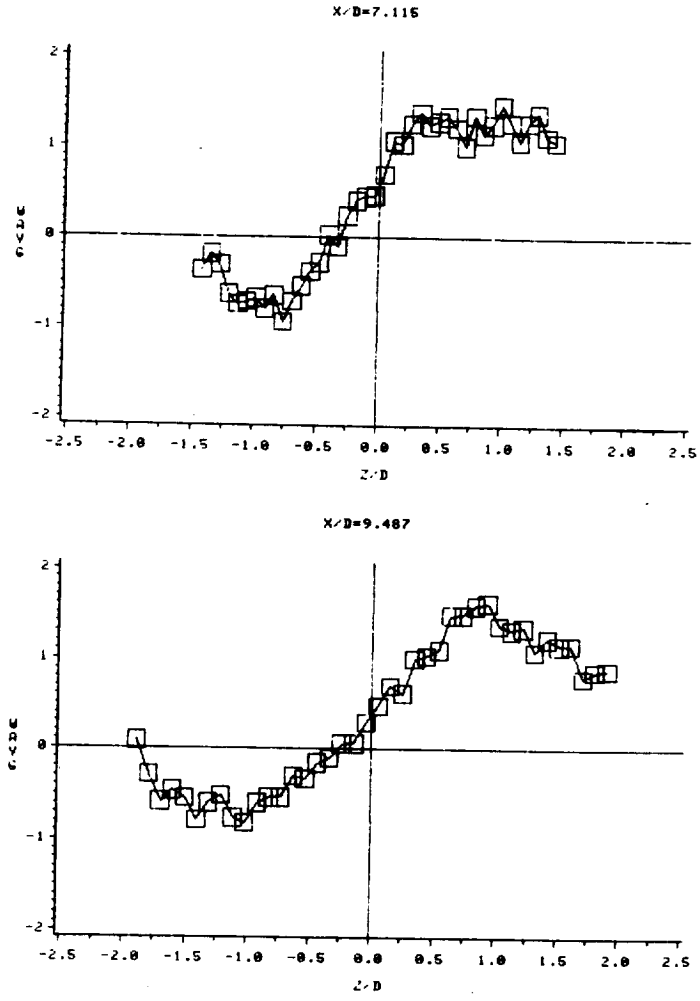

Fig. 3 Lateral profiles of mean radial velocity, V

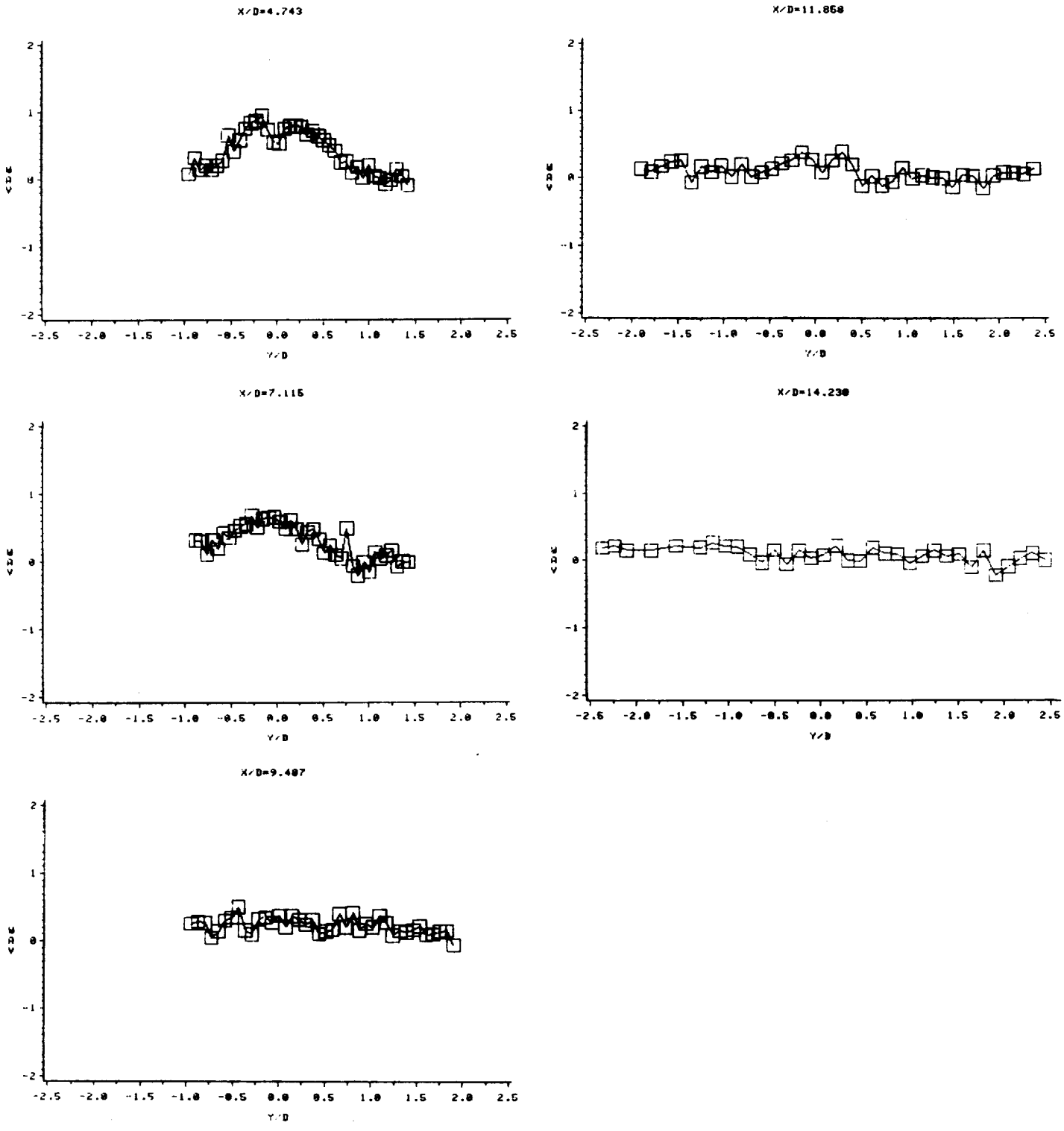

Fig. 4 Lateral profiles of mean circumferential velocity, W

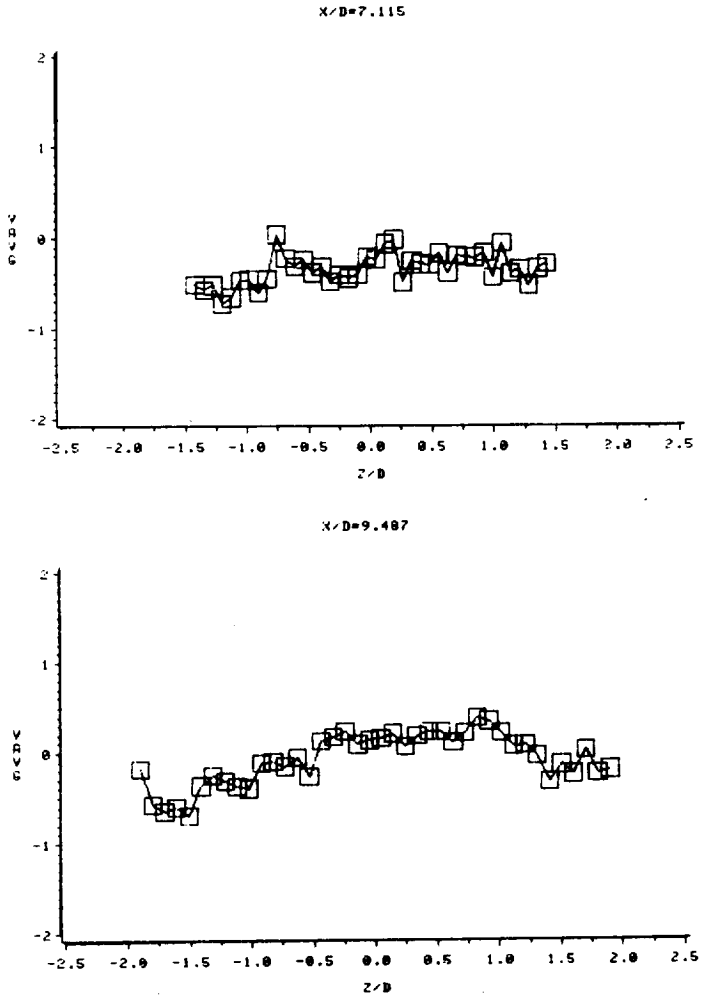

Fig. 4 Lateral profiles of mean circumferential velocity, W

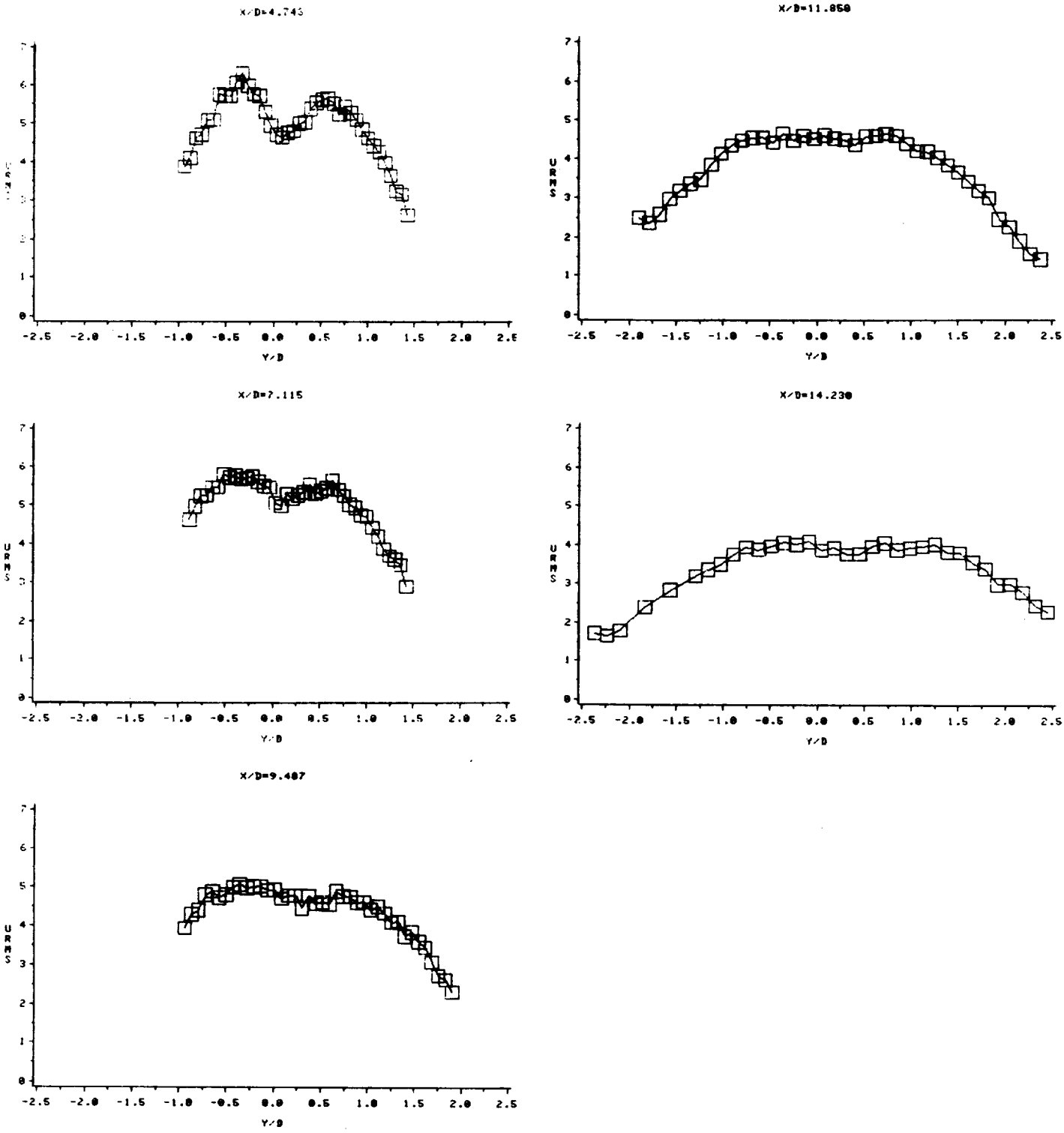

Fig. 5 Lateral profiles of RMS axial velocity, u

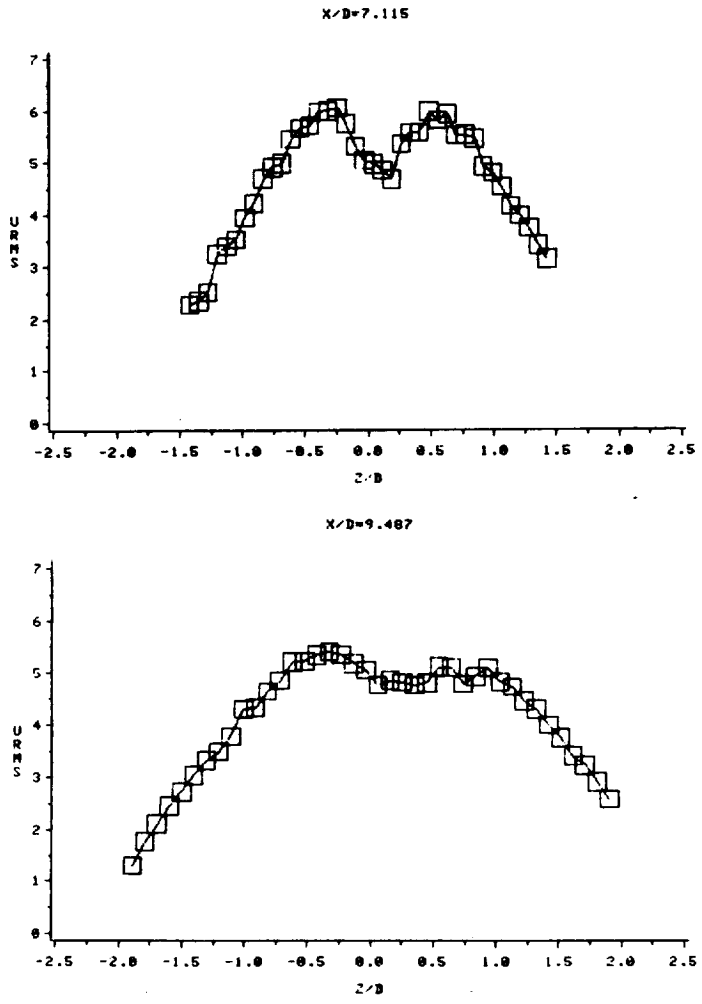

Fig. 5 Lateral profiles of RMS axial velocity, u

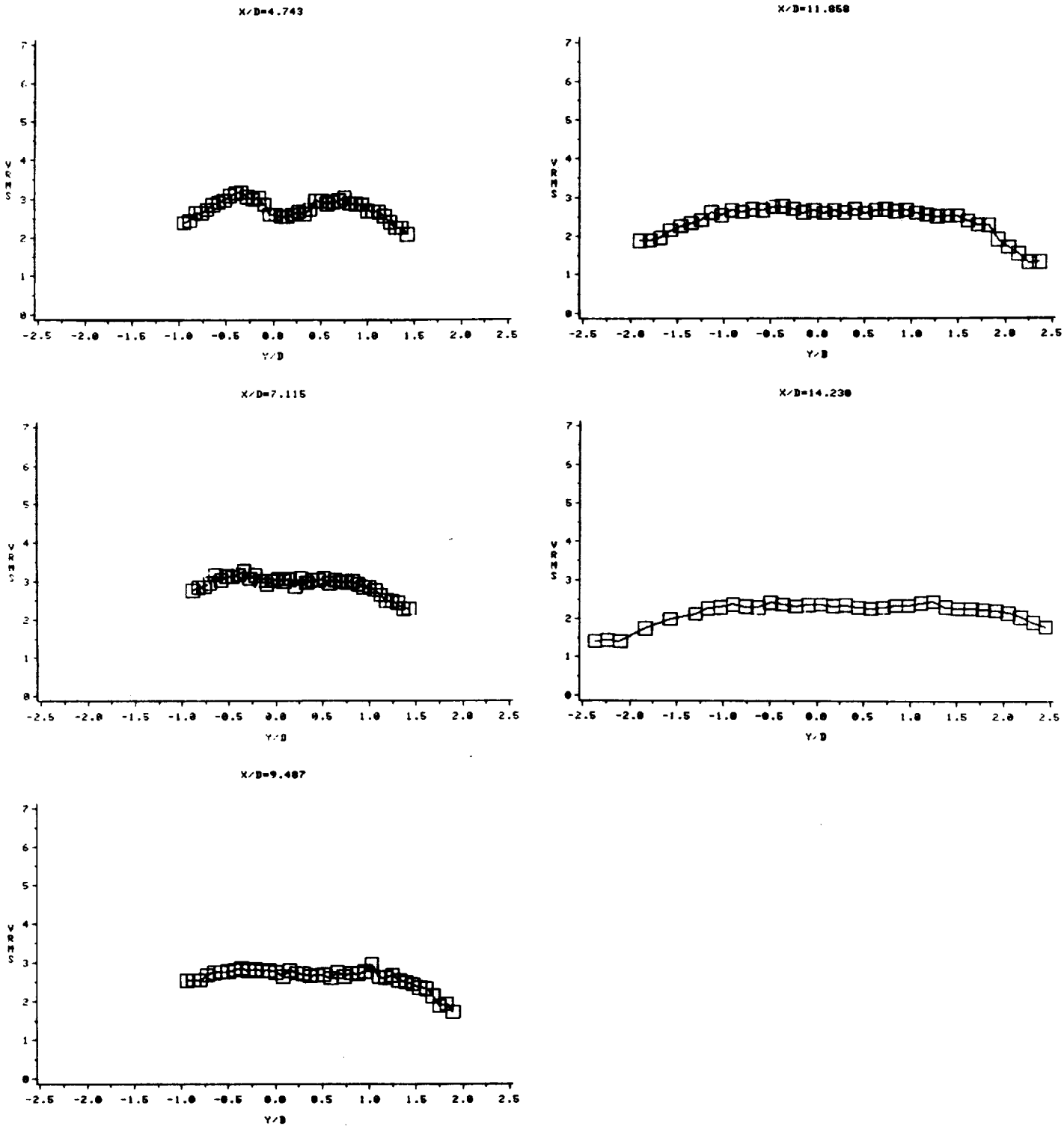

Fig. 6 Lateral profiles of RMS radial velocity, v

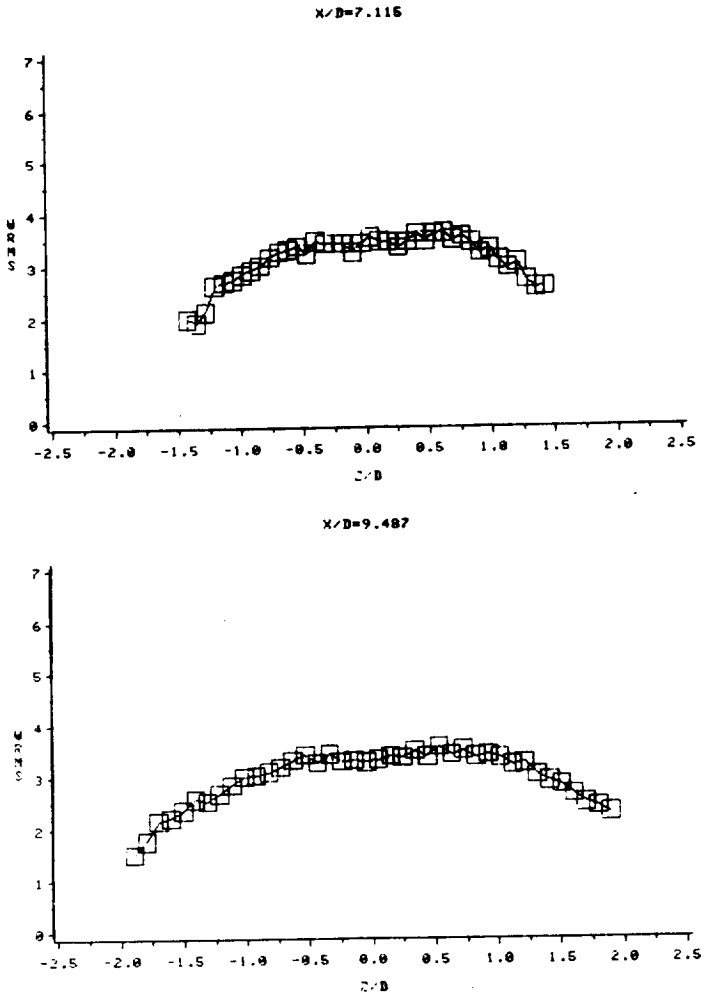

Fig. 6 Lateral profiles of RMS radial velocity, v

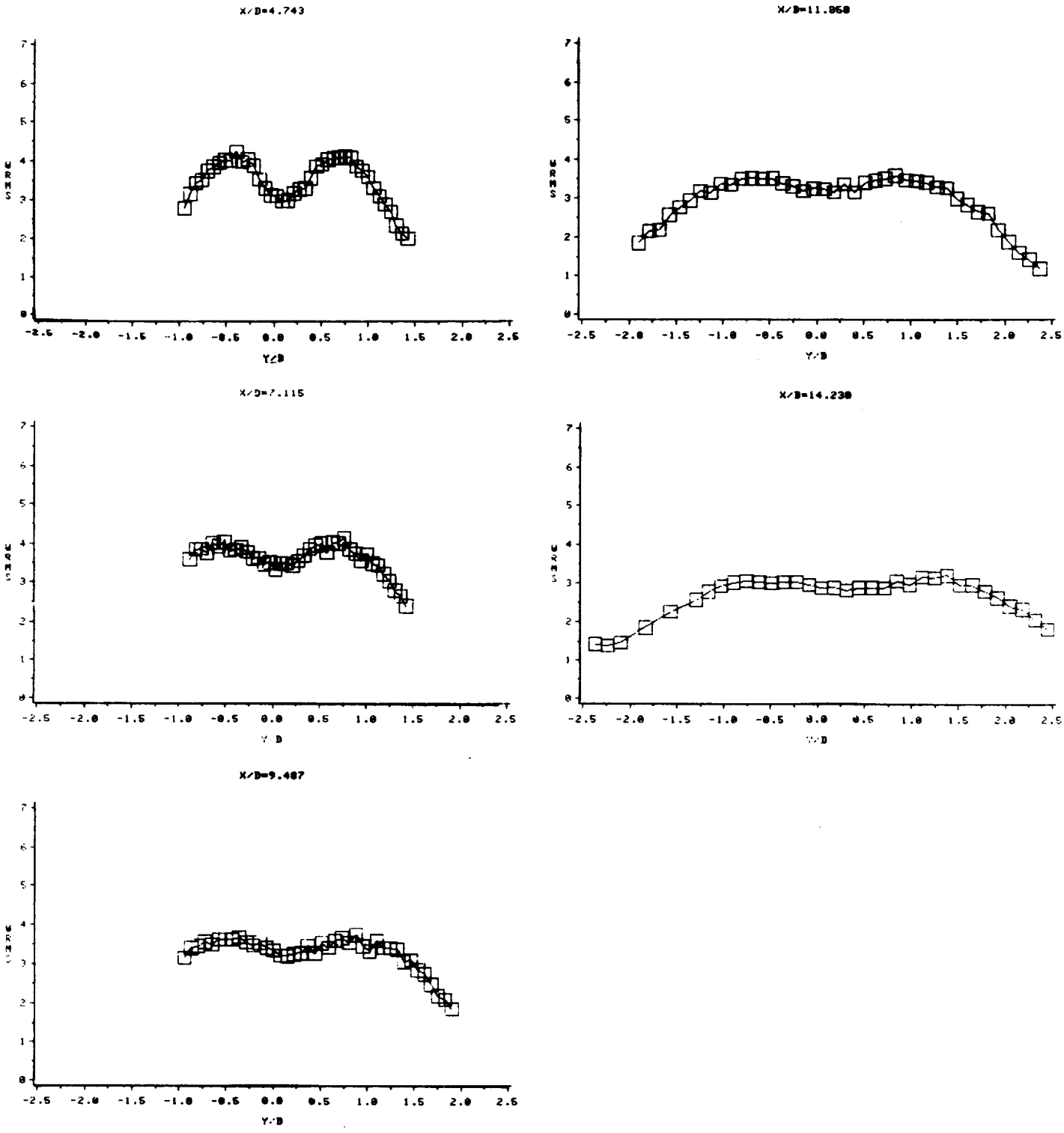

Fig. 7 Lateral profiles of RMS circumferential velocity, w

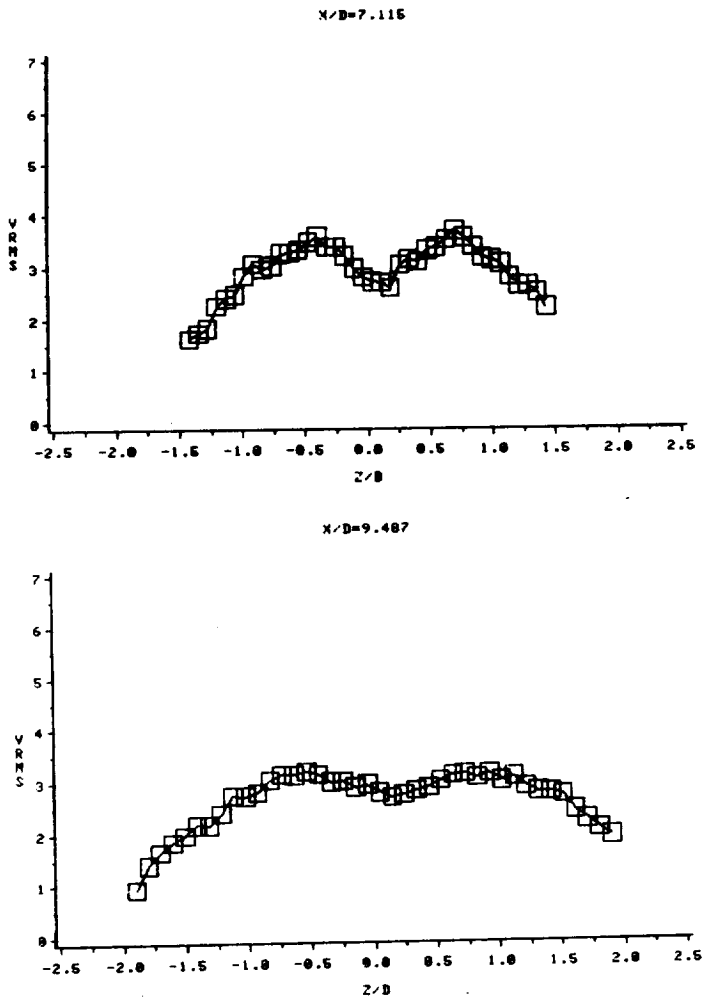

Fig. 7 Lateral profiles of RMS circumferential velocity, w

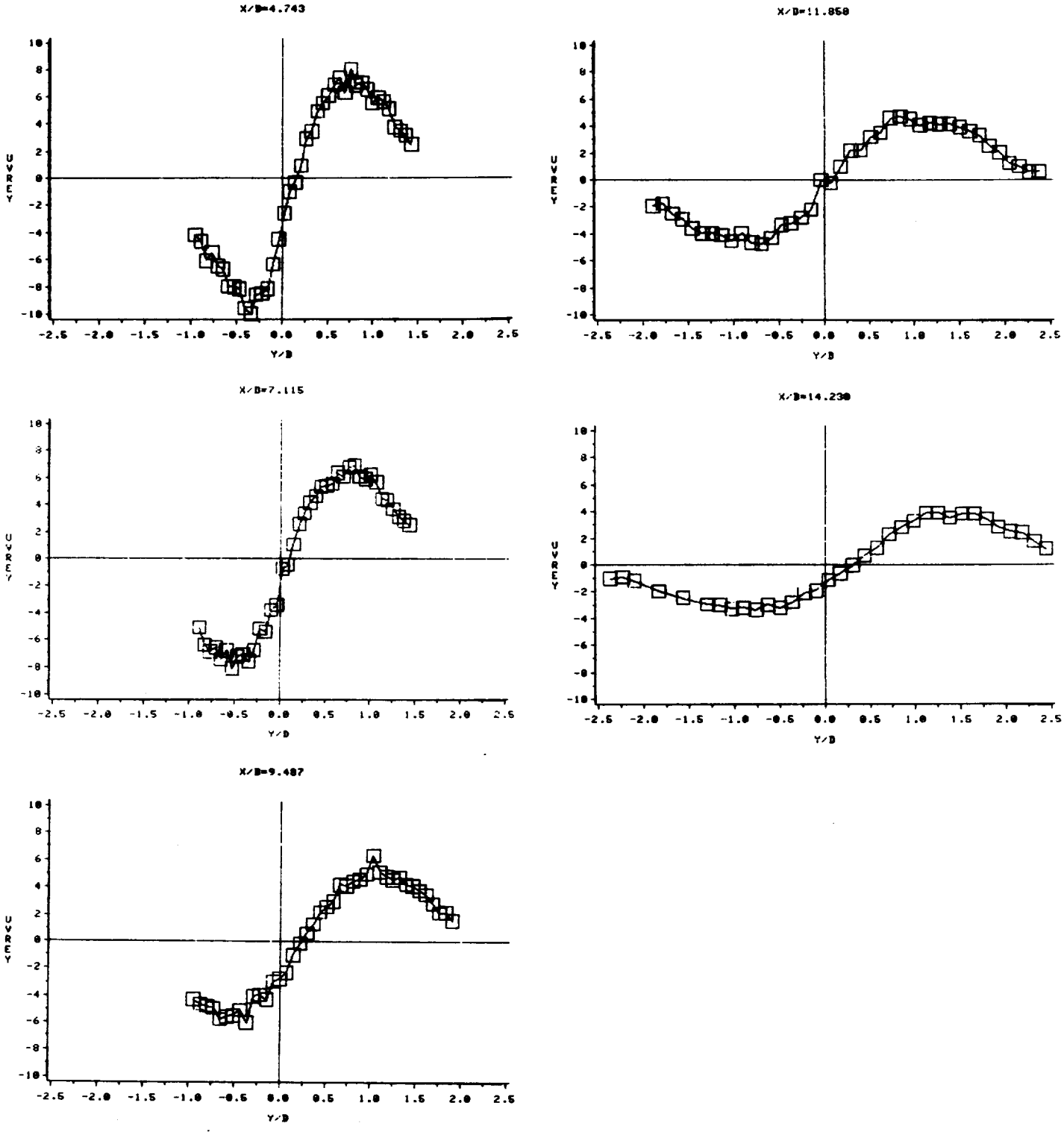

Fig. 8 Lateral profiles of $\overline{uv}$ fluctuating velocity cross-correlation

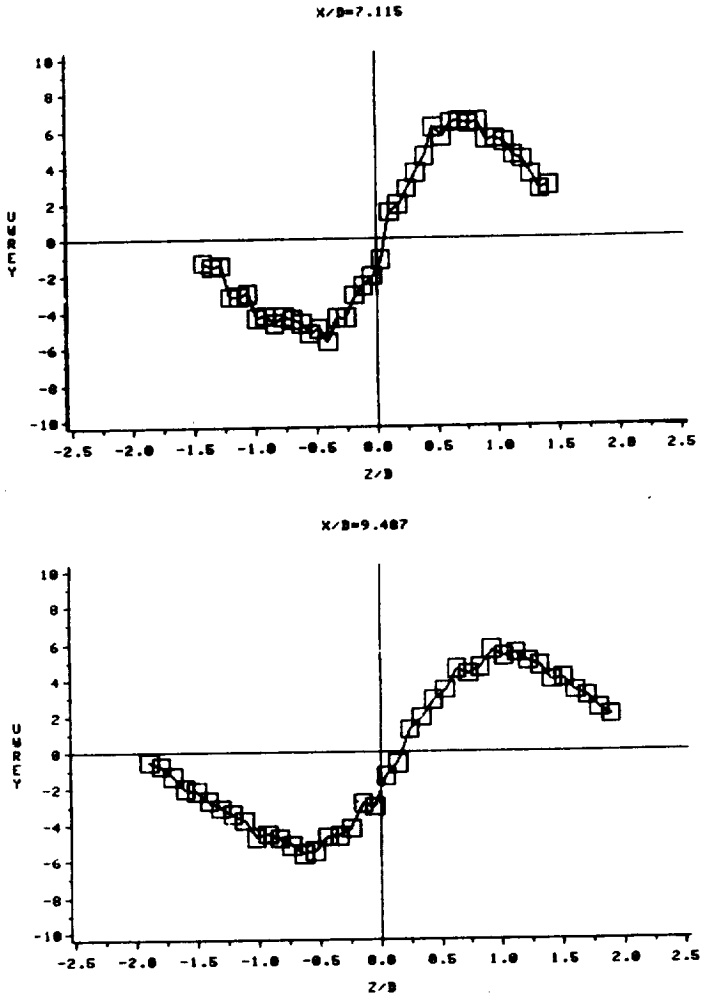

Fig. 8 Lateral profiles of $\overline{uv}$ fluctuating velocity cross-correlation

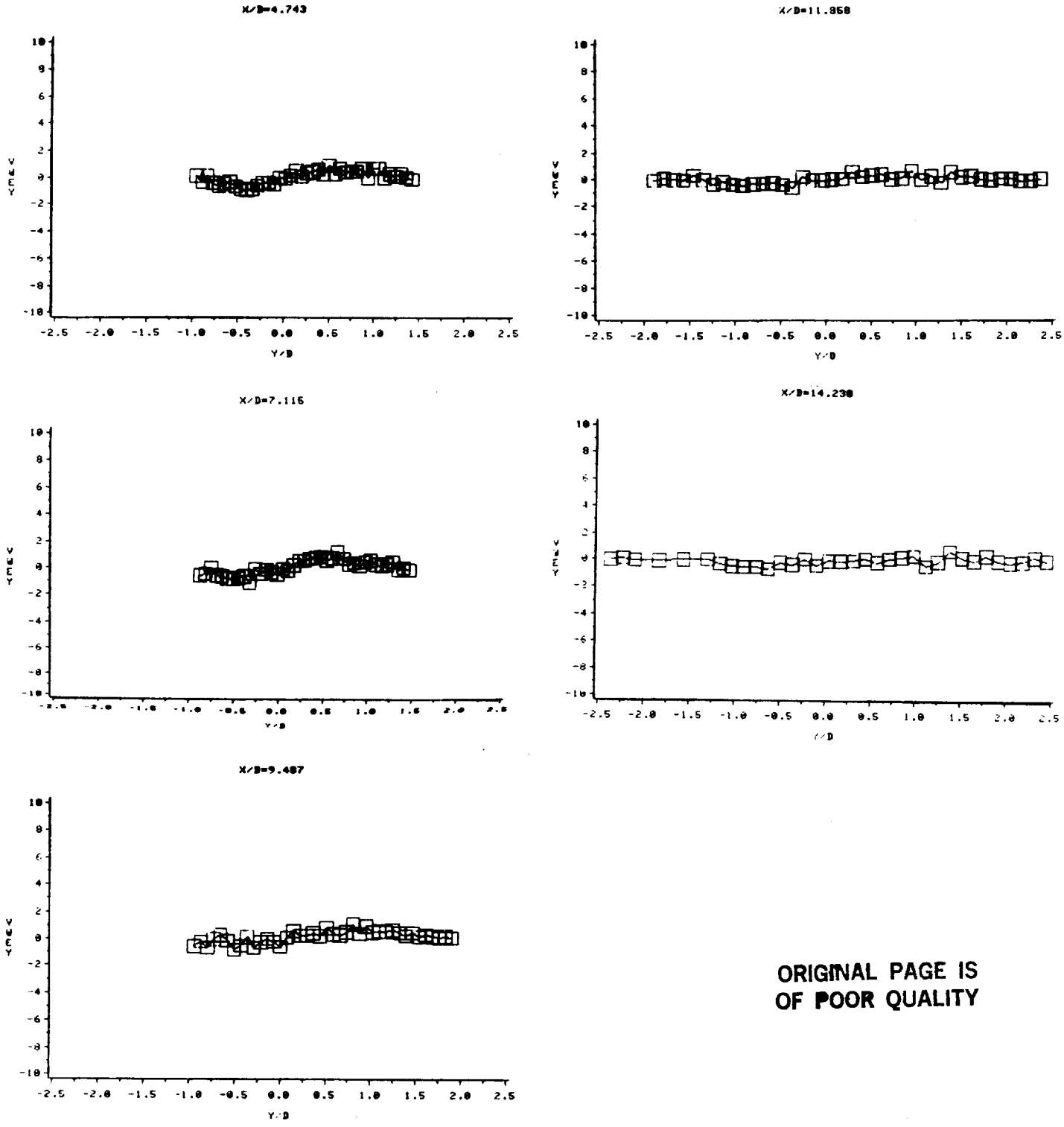

ORIGINAL PAGE IS
OF POOR QUALITY

Fig. 9 Lateral profiles of $\overline{vw}$ fluctuating velocity cross-correlation

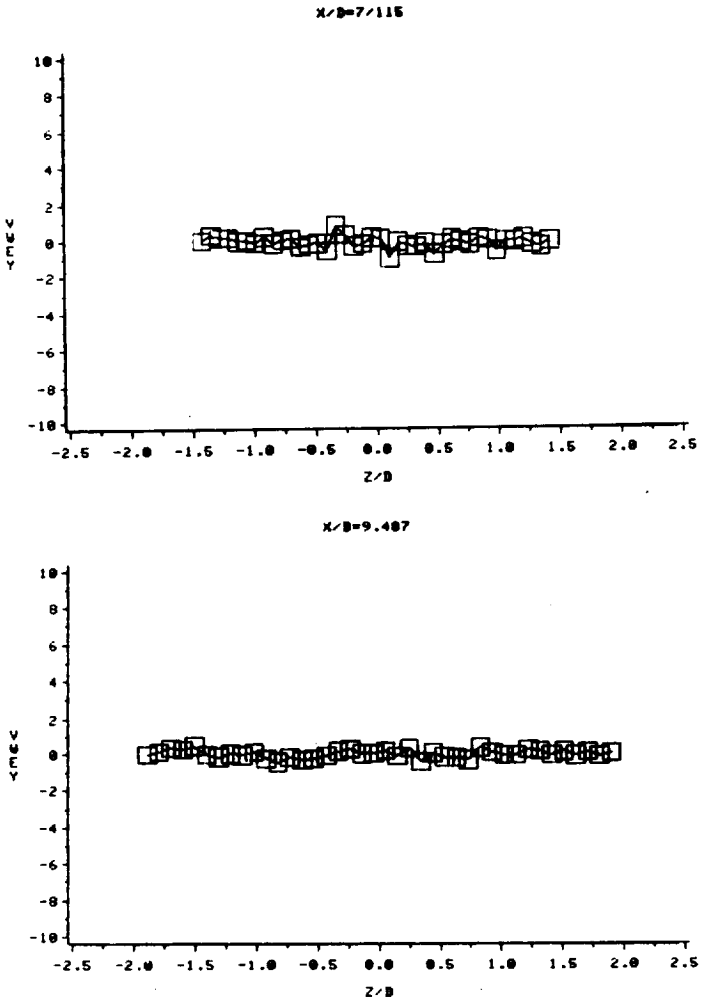

Fig. 9 Lateral profiles of $\overline{vw}$ fluctuating velocity cross-correlation

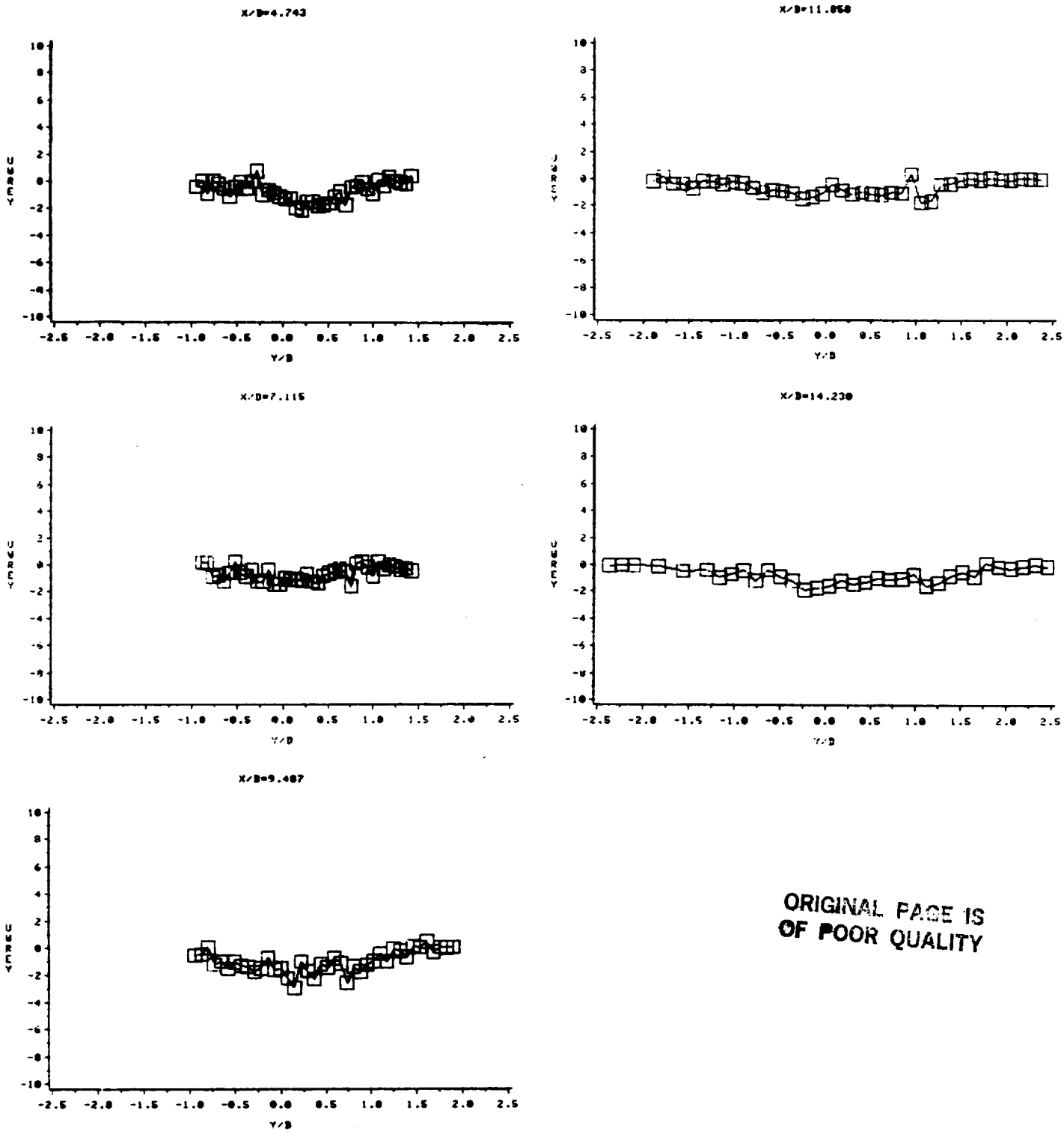

Fig. 10 Lateral profiles of $\overline{uw}$ fluctuating velocity cross-correlation

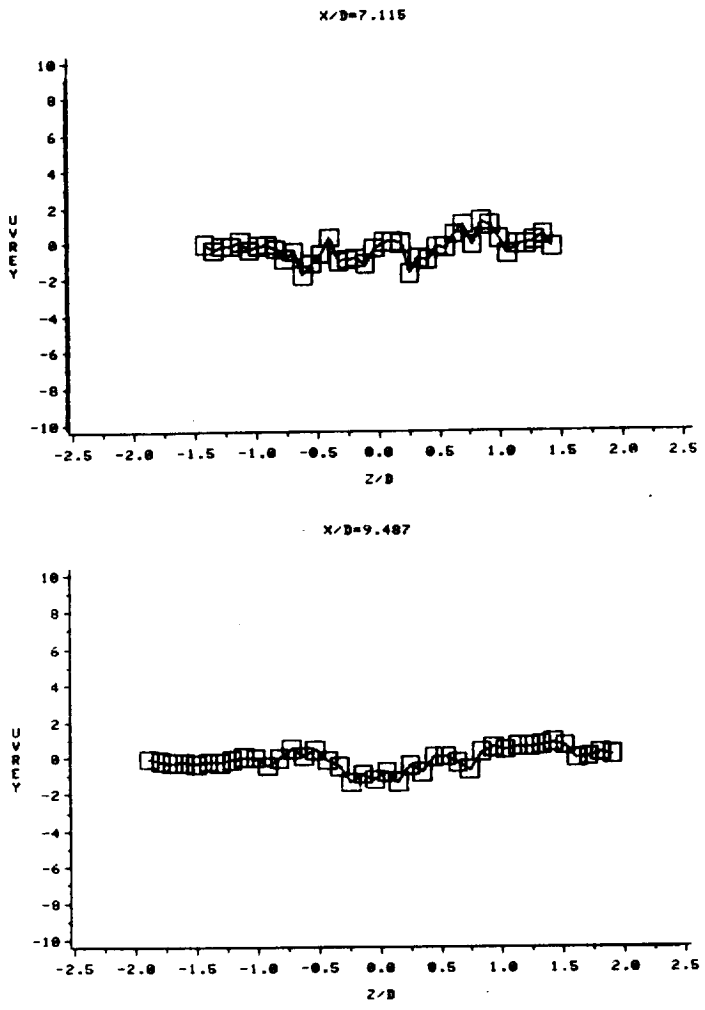

Fig. 10 Lateral profiles of $\overline{uw}$ fluctuating velocity cross-correlation

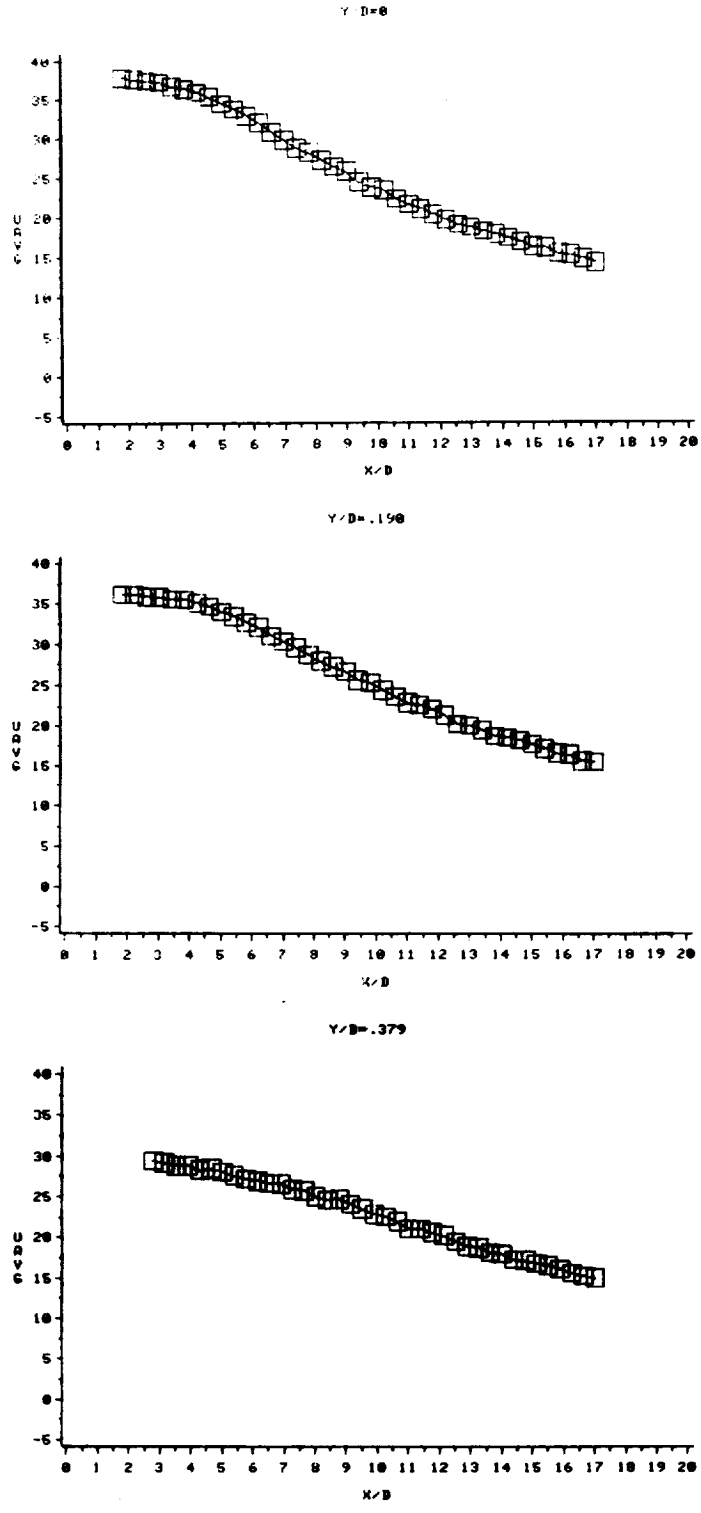

Fig. 11 Axial profiles of mean axial velocity, U

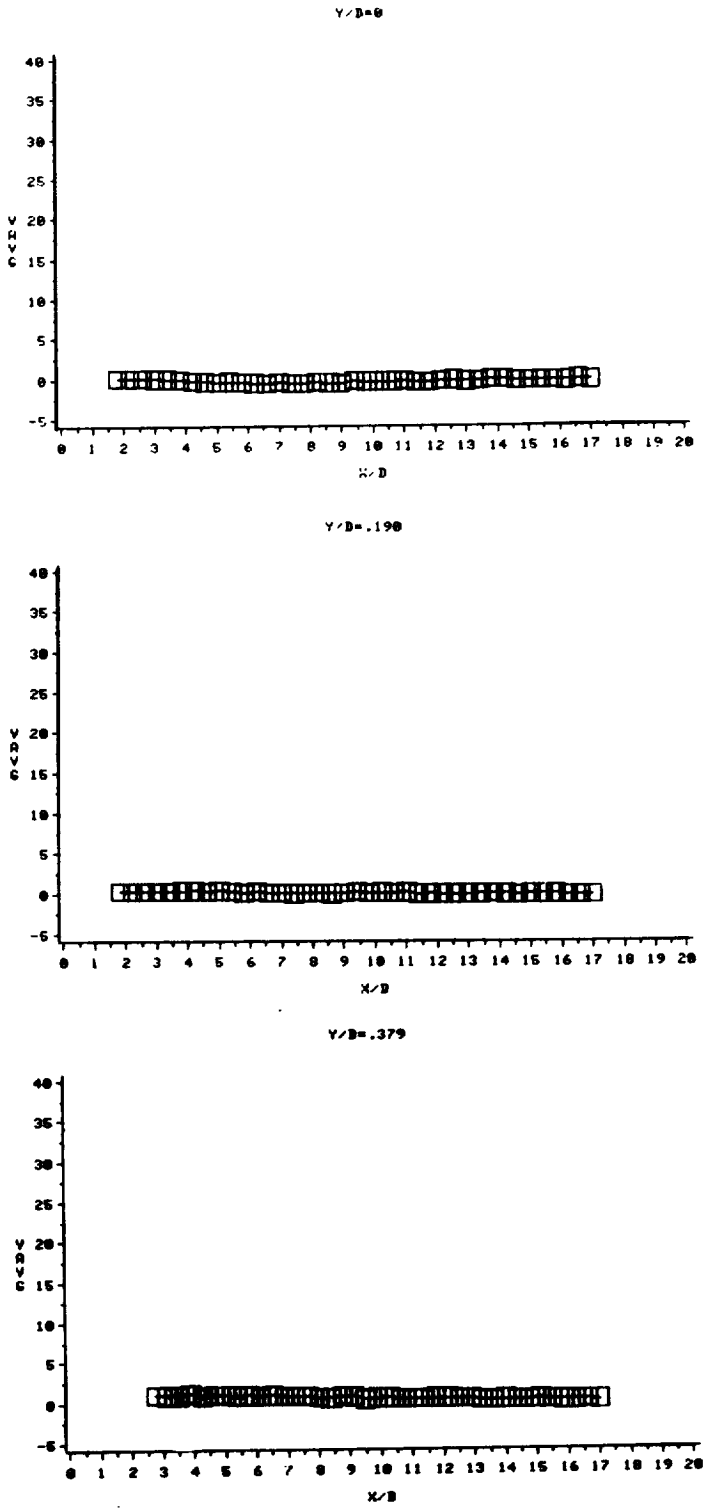

Fig. 12 Axial profiles of mean radial velocity, V

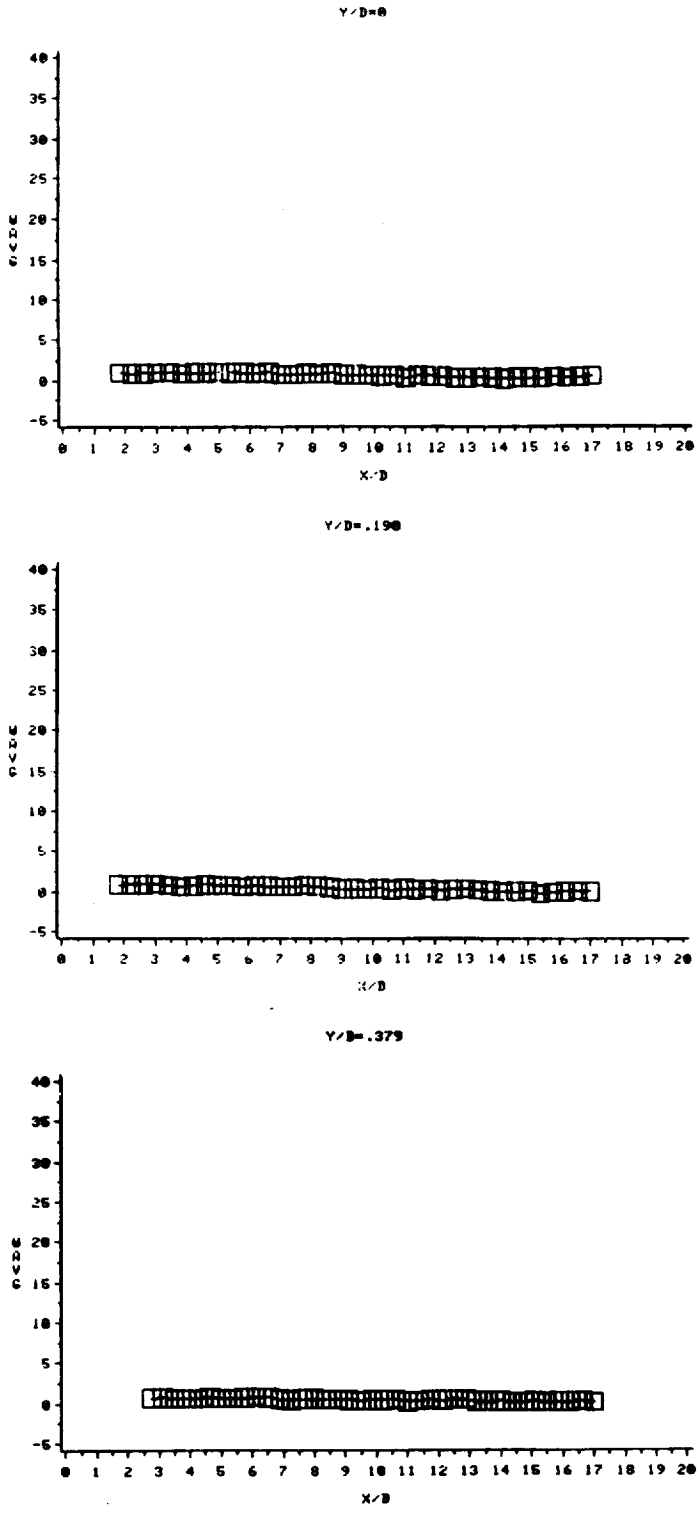

Fig. 13 Axial profiles of mean circumferential velocity, W

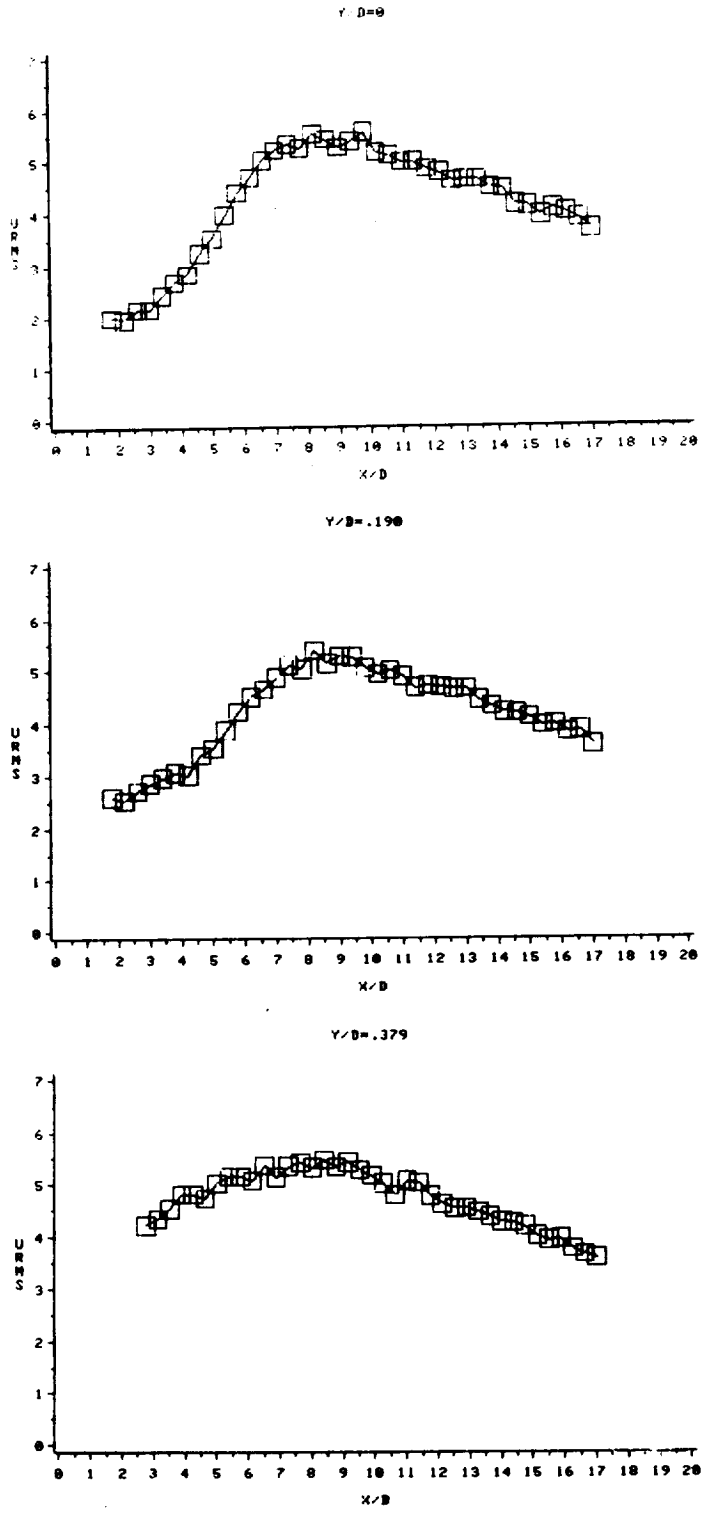

Fig. 14 Axial profiles of RMS axial velocity, u

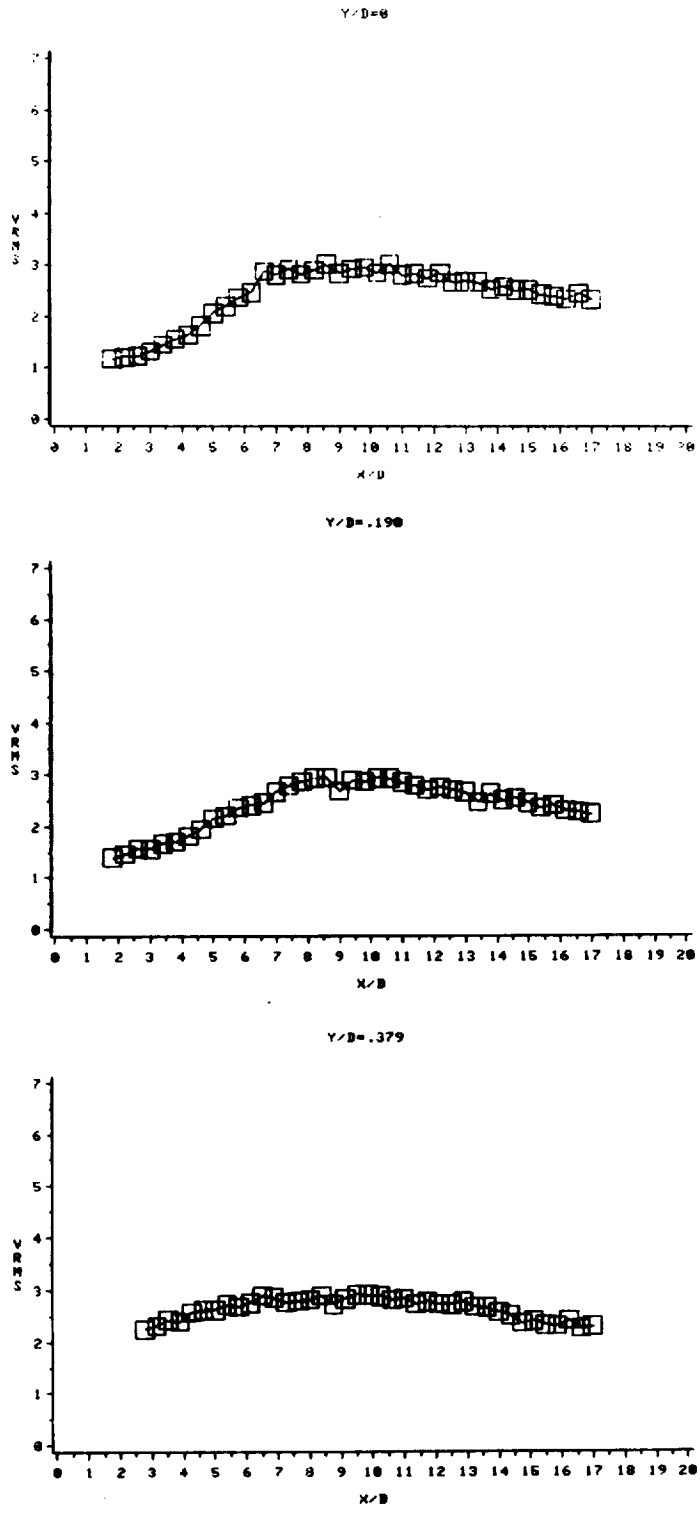

Fig. 15 Axial profiles of RMS radial velocity, v

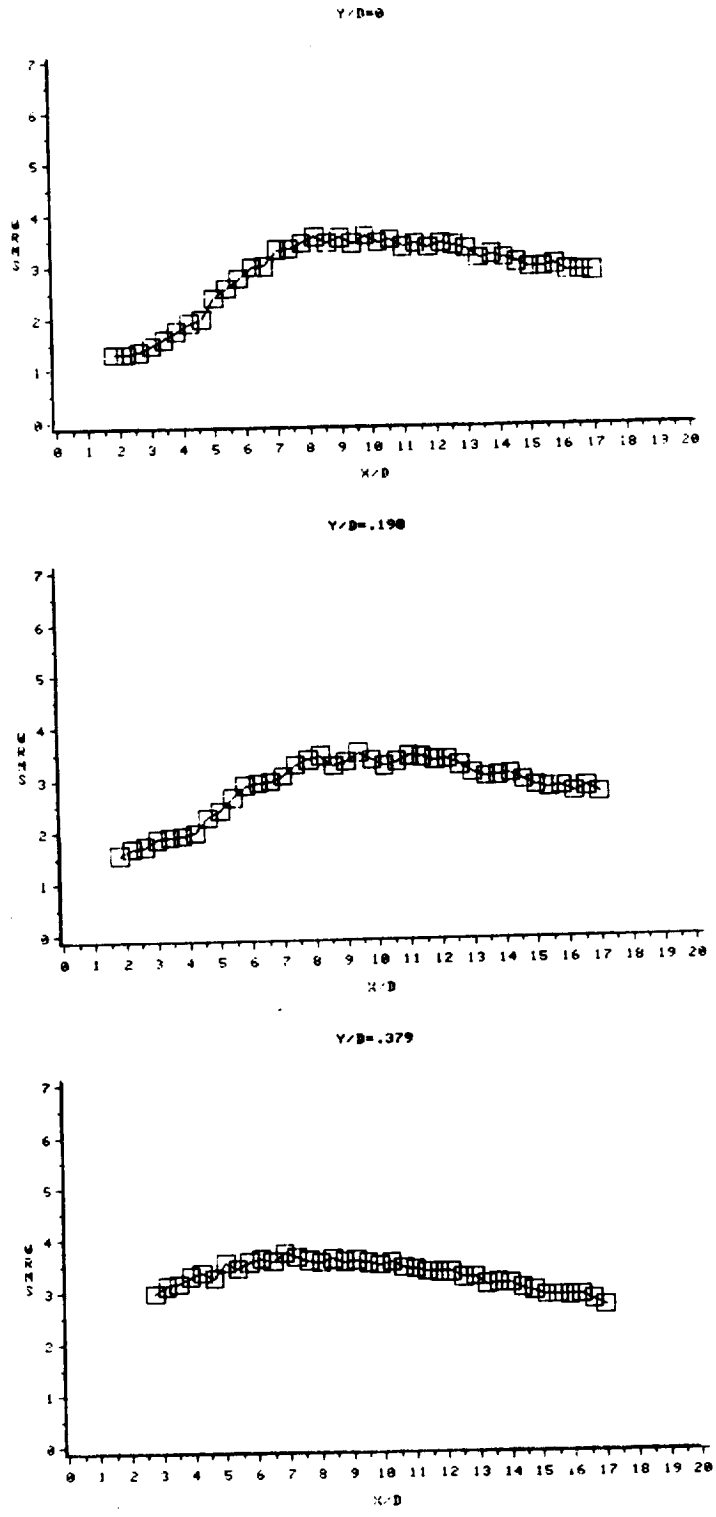

Fig. 16 Axial profiles of RMS circumferential velocity, w

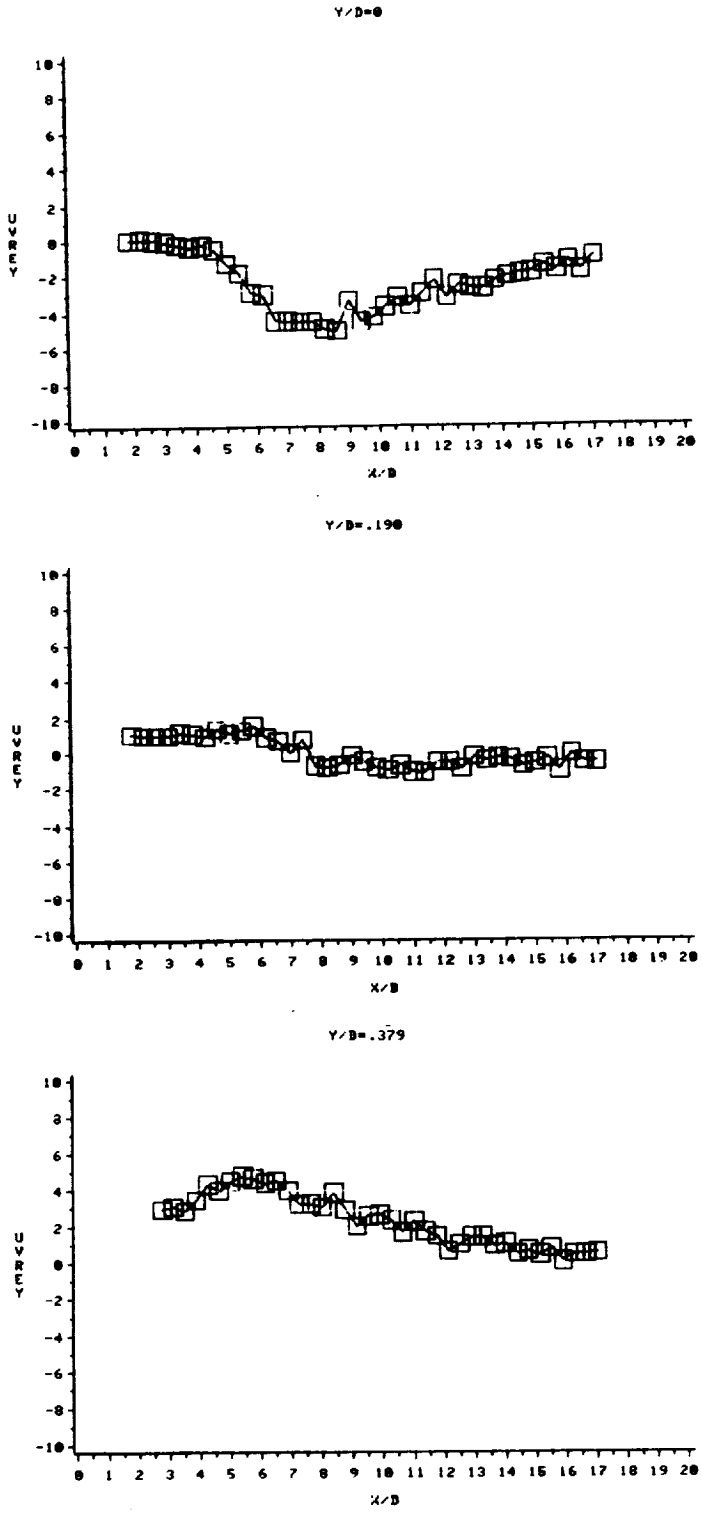

Fig. 17 Axial profiles of $\overline{uv}$ fluctuating velocity cross-correlation

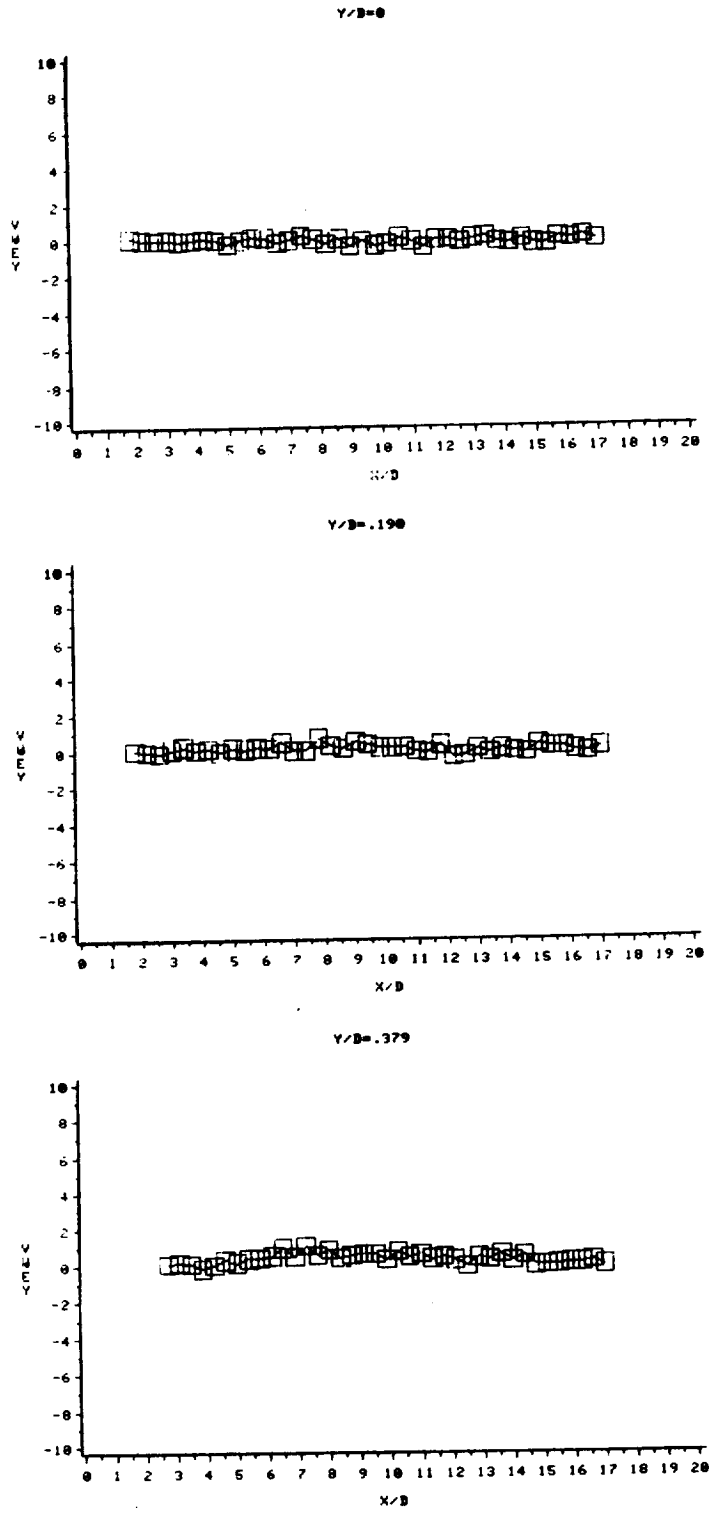

Fig. 18 Axial profiles of $\overline{vw}$ fluctuating velocity cross-correlation

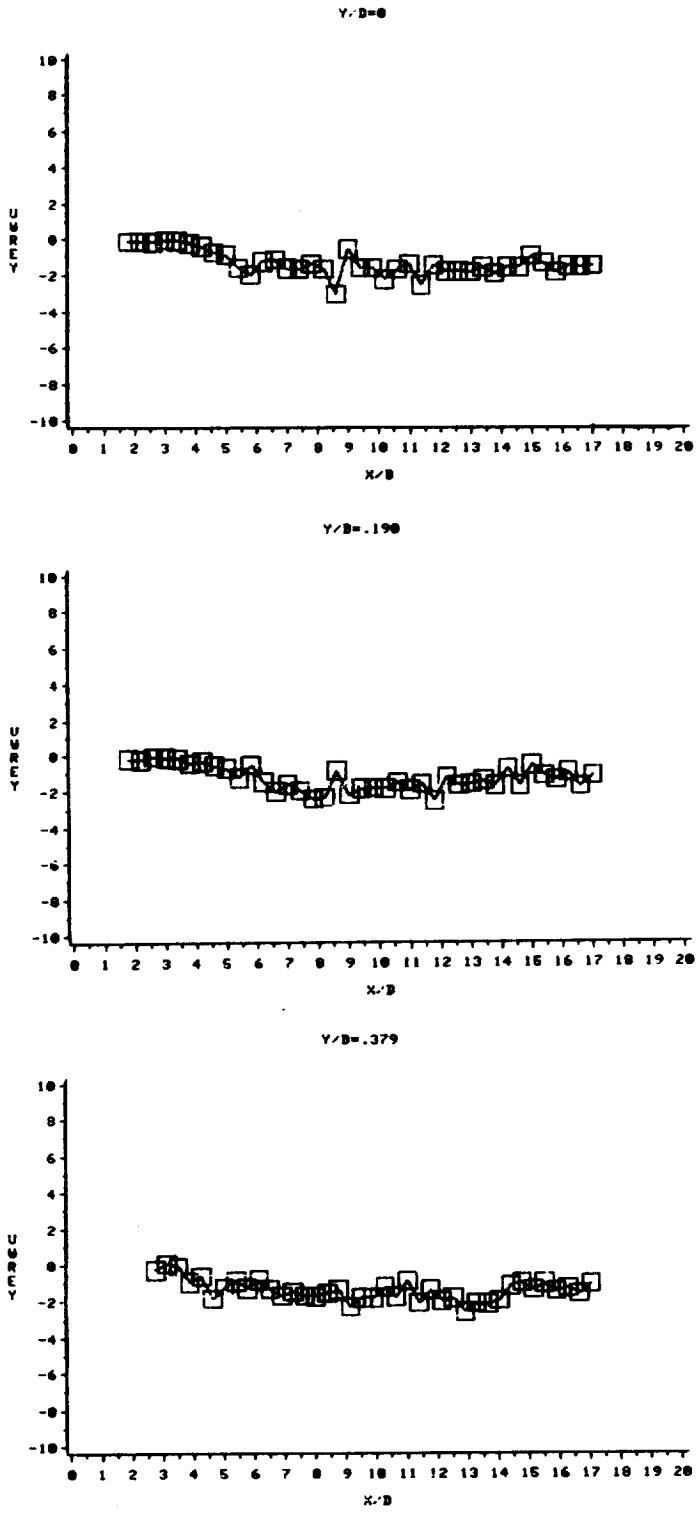

Fig. 19 Axial profiles of $\overline{uw}$ fluctuating velocity cross-correlation

NASA
National Aeronautics and Space Administration

Report Documentation Page

1. Report No.	2. Government Accession No.	3. Recipient's Catalog No.
NASA CR-181908		

4. Title and Subtitle
Three Component Laser Doppler Measurements in an Axisymmetric Jet

5. Report Date
October 1989

6. Performing Organization Code

7. Author(s)
John M. Kuhlmann
Robert W. Gross

8. Performing Organization Report No.

10. Work Unit No.
505-61-71-02

9. Performing Organization Name and Address
West Virginia University
Department of Mechanical and Aerospace Engineering
Morgantown, WV 26506-6101

11. Contract or Grant No.
NAG1-748

13. Type of Report and Period Covered
Contractor Report
May 1987-May 1989

12. Sponsoring Agency Name and Address
National Aeronautics and Space Administration
Langley Research Center
Hampton, VA 23665-5225

14. Sponsoring Agency Code

15. Supplementary Notes
Langley Technical Monitor: John W. Paulson, Jr.
FINAL REPORT

16. Abstract

A three-component laser doppler anemometer (LDA) has been used to acquire a detailed set of three-dimensional mean and fluctuating velocity measurements in a low-speed air jet entering a stagnant ambient, over the first 20 jet exit diameters along the jet trajectory. These data are physically consistent with previous measurements in axisymmetric jets. The relative difficulty of obtaining three-dimensional and two-dimensional LDA data is briefly discussed.

17. Key Words (Suggested by Author(s))
Jet Entering Still Ambient
Laser Doppler Anemometry
Turbulence
Three-Dimensional

18. Distribution Statement
Unclassified - Unlimited
Subject Category 02

19. Security Classif. (of this report)	20. Security Classif. (of this page)	21. No. of pages	22. Price
Unclassified	Unclassified	39	A03